Research on Engineering Structures & Materials

journal homepage: http://www.jresm.org

Research Group

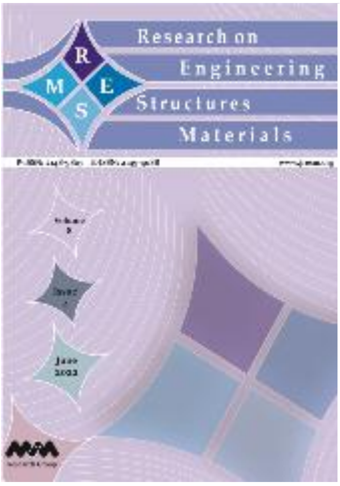

Mechanical behavior and fractography analysis of Zn-Sn alloy matrix composites reinforced with nano B4C particles

Santosh V Janamatti, Veerabhadrappa Algur, Madeva Nagaral, V Auradi

Online Publication Date: 20 March 2023

URL: http://www.jresm.org/archive/resm2022.628ma1213tn.html

DOI: http://dx.doi.org/10.17515/resm2022.628ma1213tn

Journal Abbreviation: *Res. Eng. Struct. Mater.*

To cite this article

Janamatti SV, Algur V, Nagaral M, Auradi V. Mechanical behavior and fractography analysis of Zn-Sn alloy matrix composites reinforced with nano B4C particles. *Res. Eng. Struct. Mater.*, 2023; 9(3): 885-899.

Research on Engineering Structures & Materials

journal homepage: http://www.jresm.org

MIM Research Group

Technical Note

Mechanical behavior and fractography analysis of Zn-Sn alloy matrix composites reinforced with nano B_4C particles

Santosh V Janamatti[1,a], Veerabhadrappa Algur[2,b], Madeva Nagaral[3,c], V Auradi[4,d]

[1]*Dept.t of Mechanical Eng., Ballari Institute of Technolog and Management, Ballari, Karnataka, India*
[2]*Dept. of Mechanical Eng., Rao Bahadur Y Mahabaleswarappa Engineering College, Ballari, Karnataka, India*
[3]*Aircraft Research and Design Centre, HAL, Bengaluru, Karnataka, India*
[4]*Department of Mechanical Engineering, Siddaganga Institute of Technology, Tumakuru, Karnataka, India*

Article Info

Article history:

Received 13 Dec 2022
Accepted 13 Mar 2023

Keywords:
Zn-Sn Alloy;
B_4C;
Stir Casting;
Hardness;
Tensile Strength;
Impact Strength

Abstract

The effect of nano-sized B_4C particulates on the Zn85-Sn15 alloy has been investigated. Composites reinforced with B_4C of (0%, 2%, 4% and 6%, by weight) are manufactured by two step stir casting. Microstructural studies carried out by SEM, EDS, and XRD and mechanical testing like tensile, hardness, and impact were performed on cast samples. The criteria for determining strength and fractography are met. EDS analysis confirms the homogeneous distribution of B_4C particles in the Zn-Sn matrix seen in SEM micrographs. XRD examination revealed the B_4C phases in the Zn-Sn alloy matrix as well. When B_4C reinforcement is added to the basic matrix alloy, it improves its hardness and tensile strength with slight decrease in the ductility and impact strength. Further, tensile and impact fractured surfaces were studied to know the different fracture mechanisms.

1. Introduction

Materials are the starting point for determining human age and the ability to meet daily demands. For a long time, people have had access to and used materials. We can understand that human advancements are about human usage and utilization of materials for social beneficial capacities, research, and innovation if we focus on the historical environmental variables of human growth [1].

As a novel material system, metal matrix composites (MMCs) have staked a claim in a wide variety of engineering fields. Domain-specific applications for these materials can be found in a variety of fields, such as transportation, aerospace, and medicine. Increased strength, increased stiffness, resistance to corrosion and wear, superior damping characteristics, a low coefficient of thermal expansion, etc. are just some of the properties that can be combined in metal matrix composites.

It exemplifies humanity's ability to comprehend and alter nature. When a new process for creating material is developed, the benefit will also increase dramatically, and human culture will advance [2, 3]. As a result, materials have evolved into a picture of human progress and have progressed toward being achievements for separating periods of human history. B_4C nanoparticles were supported to Zinc-compound composite using a liquid metallurgical course, in which the blending strategy was accomplished while

*Corresponding author: madev.nagaral@gmail.com
[a] orcid.org/0000-0003-2653-7239; [b] orcid.org/0000-0001-6094-6197; [c] orcid.org/0000-0002-8248-7603; [d] orcid.org/0000-0001-6549-6340
DOI: http://dx.doi.org/10.17515/resm2022.628ma1213tn

pouring the particles to avoid agglomeration of particulates and to achieve a normal homogeneous dispersion of nano particulates in the molten [4, 5].

Copper, zinc, and aluminium alloys are some of the most frequently used materials for bearing applications. These days, copper-zinc alloys and copper-tin alloys are used in a wide variety of commercial industries in place of pure copper. A lot rides on the properties constituents for MMCs to be successfully produced, used, and have their desired properties. Much of the fundamental research in MMCs has focused on the structure and behavior of the interface region. Researchers have created composites of Al, Cu, Zn, and Mg by incorporating SiC, Al_2O_3, B_4C, and graphite particles into the alloys in liquid, semisolid, and powder metallurgical forms (PM).

There are benefits to using a stir casting method, but it is still difficult to create high-quality particulate reinforced MMCs. The true challenges lie in achieving a strong bond between the Cu matrix combination and the reinforcement, limiting or avoiding the interfacial response between the framework compound and the fortification, and increasing the wettability of the fortification in the lattice material. It is common practice to add trace amounts of reactive metals like magnesium, titanium, and the like to copper melt in order to increase its wettability. In addition, wettability can be improved by employing metallic covered fortifications such as graphite, TiO_2, Al_2O_3, and SiC.

In addition, studies using B_4C as reinforcement to synthesize zinc-tin alloy with B_4C composites by liquid melt technique are extremely limited. The microstructure and mechanical properties of the prepared composites of Zn-Sn alloy with boron carbide are then analyzed.

By adding particles in preheated cast iron die by two step method. Prepared samples are machined according to ASTM principles to complete essential tests such as tensile, hardness, wear, and microstructure tests [6]. Because of its remarkable hardness, outstanding strength, high wear and impact strength, B_4C is a more prominent support material [7, 8]. The aim of this work is focusing on a wide scope of utilizations in airplane, vehicle, auto and other designing applications further writing survey uncovers that many works have been done on the utilization of micro-particles as reinforcement to blend copper-micro composites by liquid metallurgy procedure [9, 10]. The expected micro-particles molecule has thickness viable with that of aluminum and copper for all intents and purposes high hardness. Upgraded two phase mix stir cast successions is created for the composite. Delivered Zn-15Sn alloy with 500 nano size B_4C reinforcement composites are then suspended to different analyses to concentrate on mechanical and wear conduct [11, 12].

2. Experimental Details

Composites using a two-stage melt stir strategy with Zinc 85 percent-Tin15 percent wt. (Fig. 1a) were synthesized. Boron carbide particles with 2, 4 and 6 wt. % were used as the reinforcement in the Zn-Sn matrix alloy. For casting, an electric furnace with a power rating of 60 kW and a maximum temperature of 800˚C is used (Fig. 2a). A graphite crucible with the required weight percent of Zn-Sn composite network material in billet shapes was placed inside the heater and kept at a temperature of roughly 450°C. At this temperature, the entire Zn-Sn compound melted, allowing the base combination to dissolve and works out the needed wt. % of B_4C powder [13, 14].

The nano B_4C composites with Zn-Sn alloy matrix with 2% B_4C are made using a liquid metallurgy method and a stir technique. Metal ingots of a specific amount of Zn-Sn alloy are loaded into an electric furnace and heated until they melt. As, zinc-tin alloys melt at around 419˚C, but here, the molten metal has already been superheated to 450˚C. Melting and superheating temperatures are recorded using thermocouples calibrated for the appropriate temperature range. Crucibles are filled with solid hexachloroethane (C_2Cl_6) for about three minutes to degas the superheated molten metal. Zirconium ceramic is applied to a steel rotor mounted on a shaft stirrer to agitate the liquid metal. By rotating the stirrer at a speed of about 300 rpm, the molten metal is agitated to the point where a vortex is created. The stirrer is immersed in the molten metal, taking up about 60% of the depth in the crucible. In addition to stirring the molten metal, a small amount of nano B_4C particulates, equal to about 2% by weight of charged zinc-tin alloy, must be heated to about 300°C in a separate heater before being slowly poured into the molten metal vortex. Wetability between the Zn-Sn alloy matrix and the B_4C reinforcement particulates is brought to a point where interfacial shear strength can be established by continuing to stir the mixture for an extended period of time. The nano composites with a Zn-Sn and 2 wt.% B_4C composition are made by pouring a molten metal mixture containing a Zn-Sn alloy matrix and B_4C composites into cast iron moulds of 125 mm length and 15 mm diameter dimensions. Further, Zn-Sn alloy with 4 and 6 wt. % of nano B_4C reinforced composites were synthesized by similar process. Figure 2 (a-b) are showing the stir cast set up and die used to prepare composites.

(a)

(b)

Fig. 1 (a) Zn-Sn matrix (b) Nano B_4C particles

(a)

(b)

Fig. 2 (a) Stir cast set up (b) Cast iron die

For the purpose of determining whether or not reinforcing particles are distributed uniformly throughout the Zn-Sn alloy, the cast specimen is then subjected to a scanning electron microscopy (SEM) (TESCAN VEGA 3 LMU, Czech Republic) microstructural investigation. Both Zn-Sn alloy and Zn-Sn reinforced composites containing 2 to 6, wt.% of B_4C are imaged microscopically. The microstructure sample is 15mm in diameter and 5mm in height.

The specimen is machined in accordance with ASTM standard E10 [15] for hardness testing. A Brinell hardness tester (Krystal Industries, Ichalkaranji) is used to get an idea of the material's tensile strength, or how tough it is. The surface of the polished specimen is flawless. The depression is made using a ball indenter with a 5 mm diameter and 250 kg of pressure. Three indentations are made into the surface of the specimen and the results are recorded and counted.

The specimens are machined in accordance with ASTM standard E8 to investigate the tensile behavior of Zn-Sn alloy and Zn-Sn alloy with various percentages of B_4C composites. Testing tensile strength, studying the behavior of ZN-Sn alloy reinforced composites under unidirectional tension, and evaluating the uniform distribution effect are all possible with the help of a computer-measured tensile machine by Instron. This specimen measures 104 mm in total length, 45 mm in gauge length, and 9 mm in gauge diameter. This tensile test is useful for assessing the mechanical properties of composites and as cast alloys. The schematic diagram of tensile test specimen is shown in Fig. 3.

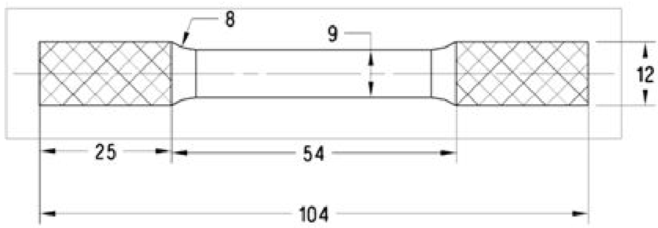

Fig. 3 Schematic diagram of tensile test specimen

Impact test is conducted by using Charpy impact testing machine. The specimen used for the impact test is shown in the Fig. 4. The test is conducted on the Zn-Sn alloy and Zn-Sn alloy with 2, 4 and 6 wt. % of nano B_4C reinforced composites as per ASTM E23 standard.

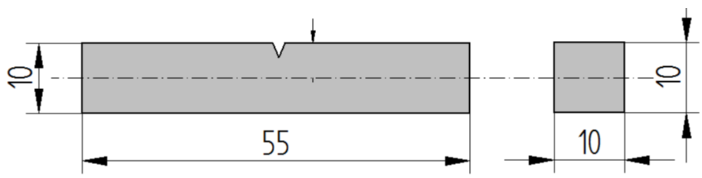

Fig. 4 Schematic diagram of impact test specimen

3. Results and Discussion

3.1. Microstructural Analysis

The microstructure of synthesized composites using as-cast Zn-Sn matrix alloy (Fig.5a), Zn-Sn-2 wt. percent B4C (Fig.5b), Zn-Sn alloy with 4 wt. percent B4C (Fig.5c), and Zn-Sn alloy with 6 wt. percent B4C composites are characterized using SEM (Fig. 5d).

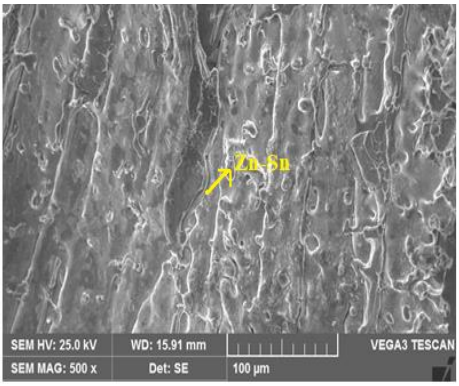

(a)

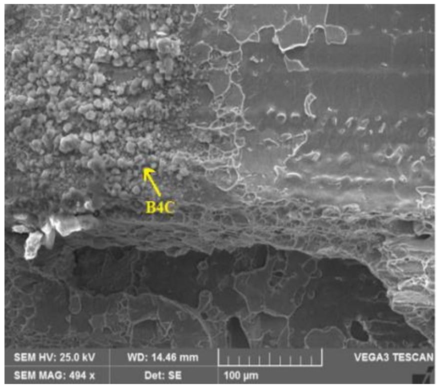

(b)

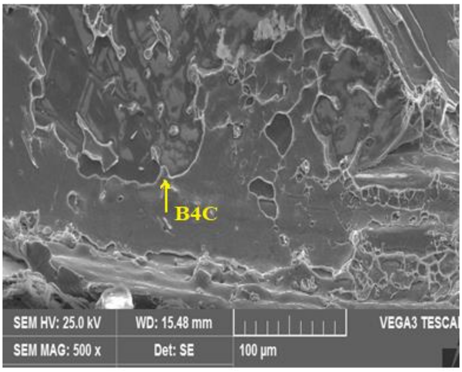

(c)

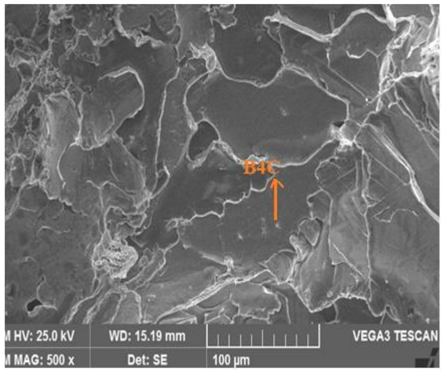

(d)

Fig. 5 SEM micrographs of (a) as-cast Zn-Sn matrix (b) Zn-Sn alloy matrix with 2 wt.% of B_4C (c) Zn-Sn alloy matrix with 4 wt. % of B_4C (d) Zn-Sn alloy matrix with 6 wt. % of B_4C composites

Fig. 5 (b-d) demonstrates the appropriation of B_4C support particulates in various wt. % of B4C, and it can be seen that the particles were dissolved finely and uniformly with no formation clustering. Furthermore, due to its sophisticated two-stage support blending method, the predicted metal grid composites show remarkably low isolation [16].

Fig. 6(a) represents the EDS of the Zn-Sn matrix whereas Fig. (b-d) can demonstrate the presence of boron particles in the Zn-Sn compound lattice. By displaying B and C materials in EDS testing, this diagram further revealed that boron and carbide components may be found in the Zn –Sn alloy matrix.

Fig. 7 shows an XRD examination of Zn-Sn alloy and Zn-Sn alloy with 6 wt. % B_4C particles (Fig. 7b). XRD investigation confirms the presence of the Sn stage over the Zn network and boron carbide stage in the Zn- Sn matrix.

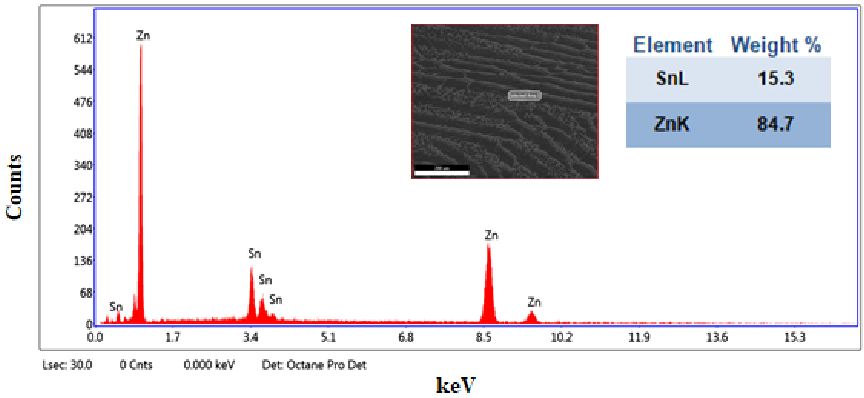
Counts
612
544
476
408
340
272
204
136
68
0
Zn
Sn
Sn
Sn
Sn
Zn
Zn
0.0
1.7
3.4
5.1
6.8
8.5
10.2
11.9
13.6
15.3
Element Weight %
SnL 15.3
ZnK 84.7
Lsec: 30.0 0 Cnts 0.000 keV Det: Octane Pro Det
keV

(a)

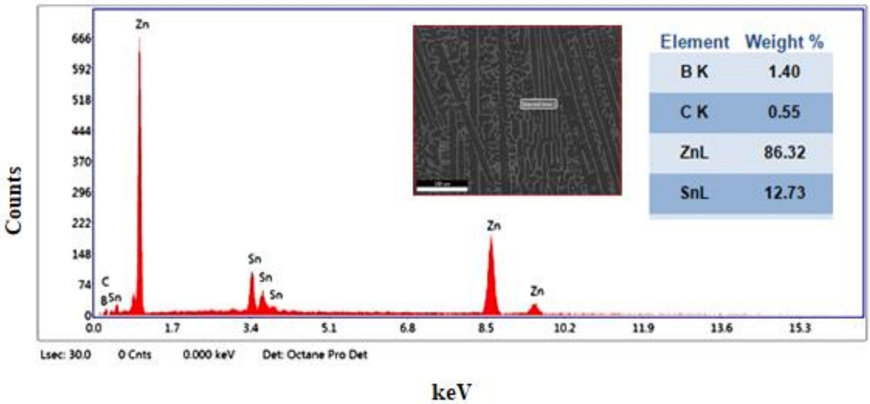
Counts
666
592
518
444
370
296
222
148
74
0
Zn
C
B Sn
Sn
Sn
Sn
Zn
Zn
0.0
1.7
3.4
5.1
6.8
8.5
10.2
11.9
13.6
15.3
Element Weight %
B K 1.40
C K 0.55
ZnL 86.32
SnL 12.73
Lsec: 30.0 0 Cnts 0.000 keV Det: Octane Pro Det
keV

(b)

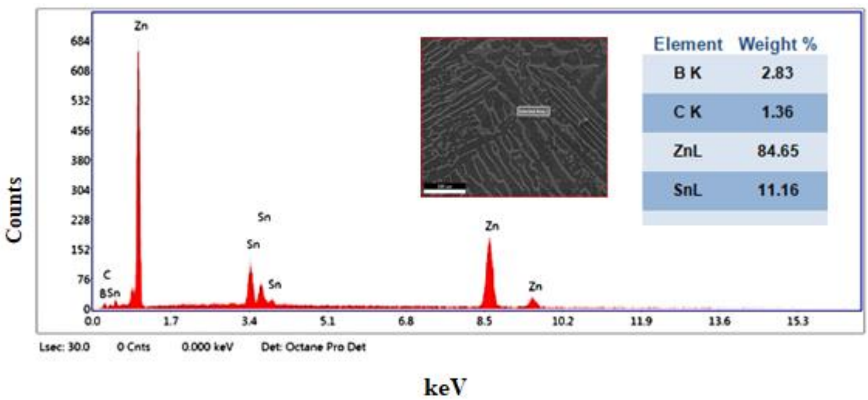
Counts
684
608
532
456
380
304
228
152
76
0
Zn
C
BSn
Sn
Sn
Sn
Zn
Zn
0.0
1.7
3.4
5.1
6.8
8.5
10.2
11.9
13.6
15.3
Element Weight %
B K 2.83
C K 1.36
ZnL 84.65
SnL 11.16
Lsec: 30.0 0 Cnts 0.000 keV Det: Octane Pro Det
keV

(c)

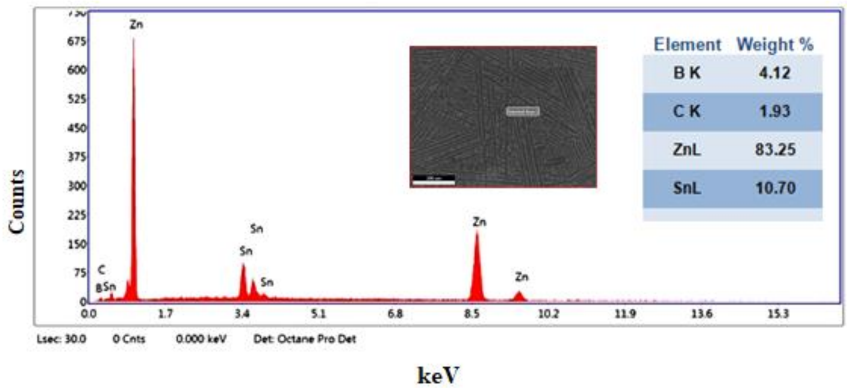

(d)

Fig. 6 EDS spectrums of (a) as-cast Zn-Sn matrix (b) Zn-Sn alloy matrix with 2 wt.% of B_4C (c) Zn-Sn alloy matrix with 4 wt. % of B_4C (d) Zn-Sn alloy matrix with 6 wt. % of B_4C composites

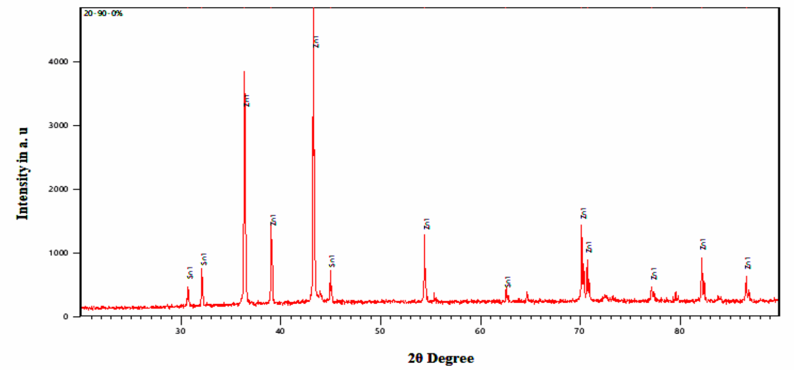

(a)

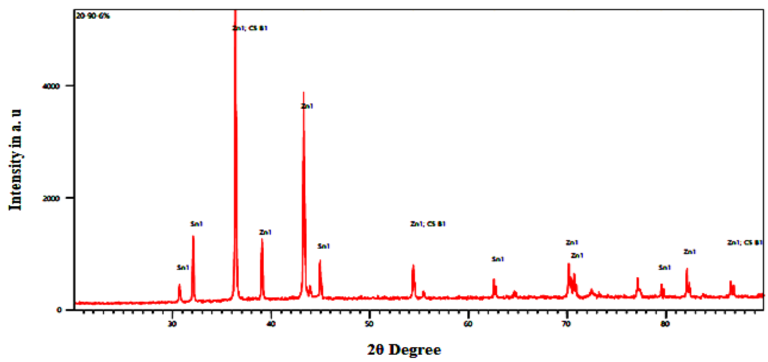

(b)

Fig. 7 XRD patterns of (a) as-cast Zn-Sn matrix (b) Zn-Sn alloy matrix with 6 wt. % of B_4C composites

3.2. Hardness Measurements

Hardness benefits from a combination of Zn-2, and 6wt. % in the current research. Brinell hardness analyzer has found percent B_4C composites. Fig. 8 shows the hardness of Zn-2, 4& 6, wt% of B_4C composite is higher than Zn basis matrix in terms of percentage [17]. With increasing of B_4C particles, a significant increase in the composite matrix hardness can be detected. The presence of B_4C particles in the framework Zn alloy is the main reason for this. The hardness of the composite material is improved whenever firm reinforcement is consolidated into a delicate base alloy. As can be seen in Figure.8, the Brinell hardness increases as the B_4C particles are increased. The tougher particles are responsible for the increase in hardness [18].

Table 1. Hardness of Zn-Sn alloy and its nano B_4C composites with standard deviation

Material Composition	Hardness (BHN)
Zn-Sn Alloy	82.03 ± 1.50
Zn-Sn – 2 wt. % B_4C	88.53 ± 1.43
Zn-Sn – 4 wt. % B_4C	100.20 ± 1.15
Zn-Sn – 6 wt. % B_4C	115.02 ± 1.16

± - SD (Standard Deviation)

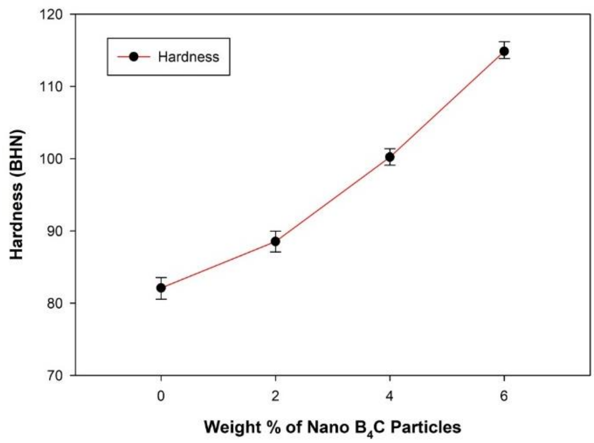

Fig. 8 Hardness of Zn-Sn alloy and its nano B_4C composites

3.3. Tensile Properties

Fig.9 shows the ultimate strength (UTS) and yield strength (YS) for Zn alloy, and 2, 4 and 6 wt. percent B_4C composites. The proximity of hard B_4C particles is credited with the improvement in ultimate and yield strength.

Ultimate and yield strength of as-cast Zn alloy with 2, 4 & 6 wt. % B_4C reinforcement, as illustrated in the Fig. 9. Boron carbide particles enhanced the yield Strength of the base matrix. Zn-Sn combination. In a fine Zn composite base network, ceramic particles are uniformly combined [19]. Many ceramics, such as boron ceramics, will resist external weight in contrast to delicate materials, and as a result, they will not twist plastically successfully, increasing their yield resistance rate.

The tensile properties of these materials might be affected by the consistency of the particle dispersion. It has been demonstrated that these are currently quite homogeneous, so it is anticipated that they will not significantly affect the trends of the current work. Clusters can cause localized damage that compromises a material's strength and ductility. In this sense, such aggregations may be viewed as pre-loading danger zones. It is important to note that clustering is often more prevalent in composites reinforced with small particulates, despite the fact that these composites appear to have greater strength and ductility than materials containing coarse particles. Any areas of clustering must be kept to a minimum if top performance is desired, and this is especially true for nanoparticle-reinforced composites.

Table 2. Tensile properties of Zn-Sn alloy and its B_4C composites with standard deviation

Material Composition	Ultimate Tensile Strength (MPa)	Yield Strength (MPa)
Zn-Sn Alloy	315.15 ± 1.54	248.37 ± 1.21
Zn-Sn – 2 wt. % B_4C	330.32 ± 1.12	266.86 ± 1.33
Zn-Sn – 4 wt. % B_4C	357.44 ± 1.39	295.09 ± 0.97
Zn-Sn – 6 wt. % B_4C	394.46 ± 0.56	326.03 ± 0.94

± - SD (Standard Deviation)

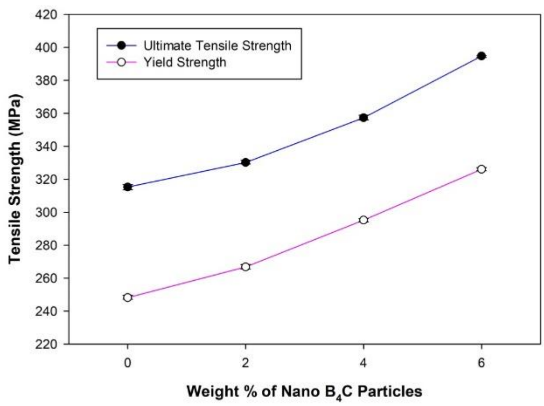

Fig. 9 Ultimate and yield strength of Zn-Sn alloy and its nano B_4C composites

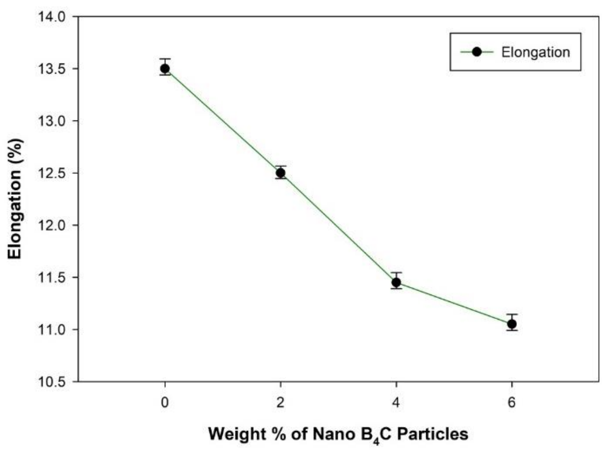

Fig. 10 Elongation of Zn-Sn alloy and its nano B_4C composites

Elongation of as-cast Zn composite with 2, 4 6 wt. % of B_4C reinforcement is shown Fig. 10. It was shown that as boron carbide particles increased in base matrix the % of elongation is reduced, as shown in Figure.11. Harder particles are consistently integrated into the Zn-Sn base alloy [20]. Due to two step stir action hard boron carbide particles are distributing uniformly throughout the base solution, hence substitution solid solution was achieved. As results, boron is influencing on delicate base alloy, then base alloy successfully opposes plastically, increasing yield strength rate and diminishes the machinability and % of elongation.

Fig. 11 (a-d) are representing stress-strain graphs of as cast Zn-Sn alloy, Zn-Sn alloy with 2, 4 and 6 wt. % of nano B_4C reinforced composites. Boron carbide reinforced Zn-Sn alloy composites exhibited superior load carrying capacity as compared to the as cast Zn-Sn alloy. The ultimate tensile stress of as cast Zn-Sn alloy is 311115 MPa, as weight percentage of B_4C particles content increased in the Zn-Sn alloy, the tensile strength incraesed. Zn-Sn alloy with 2, 4 and 6 weight % of boron carbide reinforced composites exhibits 330.32 MPa, 357.44 MPa and 394.46 MPa respectively with reduced strain. The increase in load carrying capacity with addition of B_4C is mainly due to the load bearing capacity of hard carbide particles during tensile laoding onditions.

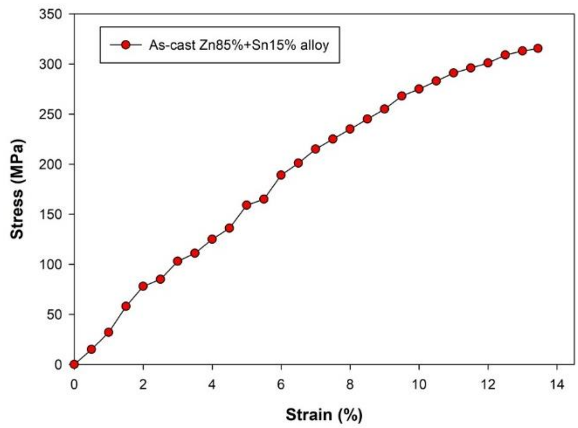

(a)

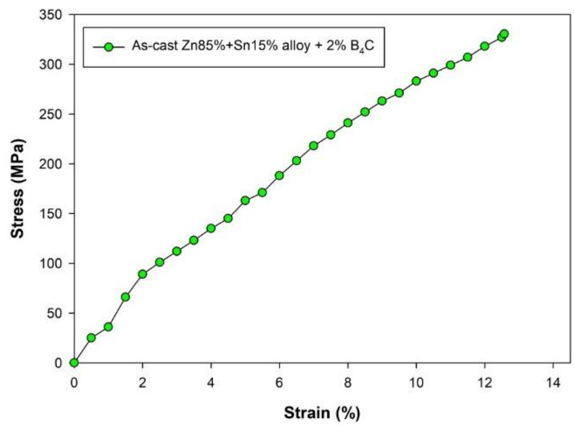

(b)

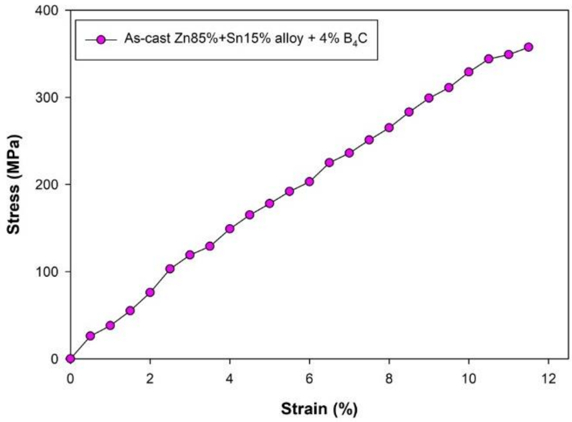

(c)

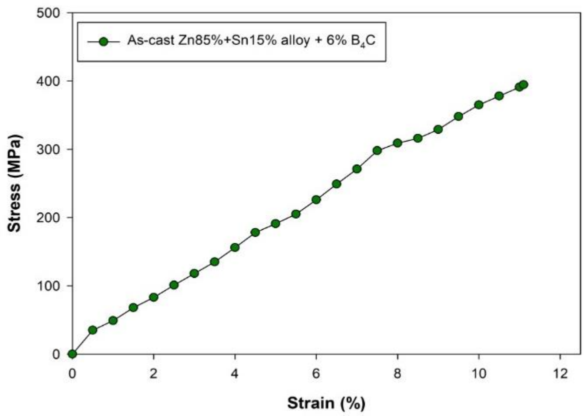

(d)

Fig. 11 Stress-strain graphs of (a) as-cast Zn-Sn matrix (b) Zn-Sn alloy matrix with 2 wt.% of B_4C (c) Zn-Sn alloy matrix with 4 wt. % of B_4C (d) Zn-Sn alloy matrix with 6 wt. % of B_4C composites

3.4. Tensile Fractography

Fig. 12 shows the tensile fractured surfaces of as-cast Zn alloy and Zn-Sn alloy with 6 wt. percent of B4C composites (a-b). The goal of the tensile fracture surfaces research is to see how boron carbide particles alter Zn alloy fracture behavior [21]. The particles were equally distributed throughout the matrix alloy in the current investigation, boosting microhardness, ultimate, and yield strength while lowering ductility. Interfaced cohesion between the Zn –Sn alloy matrix and B4C particles, reinforcement fracture, and matrix failure are all causes of failure in particle-reinforced metal composites [22].

The as-cast Zn alloy's tensile cracked surface in Fig. 12 (a) shows larger and more uniform dimples, indicating malleable fracture. On the cracked surfaces of Zn alloy reinforced with 6 wt .% of B_4C particles (Fig.12b), the size dimples are less than on the as-cast Zn matrix. On the fracture surfaces of composites, electron microscopy revealed particle decohesion with the matrix and reinforcement [23]. The particle fracture is less ductile in the majority of cases, and the surface is smooth and crisp, showing that the particle is broken rather than decreased, implying that high interface strength dominates these composites.

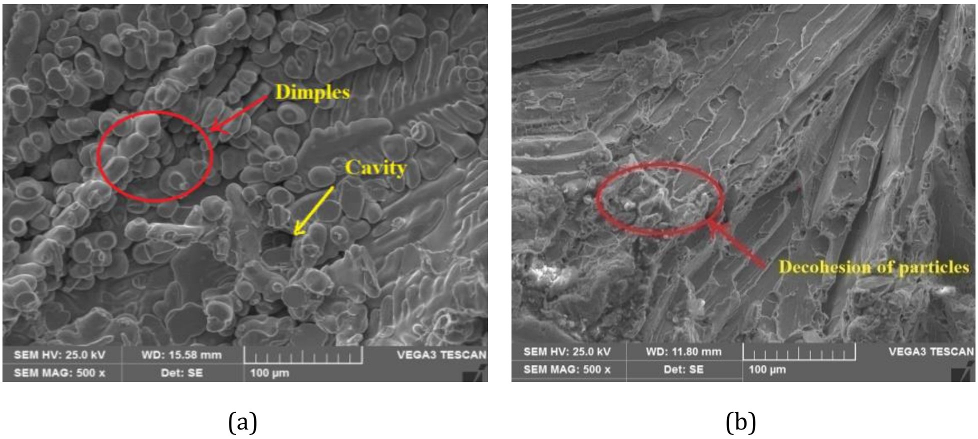

Fig. 12 Tensile fractured surfaces SEM images of (a) as-cast Zn-Sn matrix (b) Zn-Sn alloy matrix with 6 wt. % of B_4C composites

3.5. Impact Strength and Fractography

The impact strength of Zn alloy reinforced metal composites containing 2 to 6 wt.% B_4C particles is shown in Fig 13. The impact strength of Zn alloy as-cast is 3.5 J, but the impact strength of Zn-Sn alloy with 2, 4 and 6 wt.% of B_4C composites are 3.0, 2.49 and 2.0 J respectively with the addition of ceramic particles. Because of the hard particle and matrix contact, composites absorb less energy than as-cast Zn matrix. The creation of a hard interface between the matrix and reinforcement is influenced by load transfer, which is critical for improving composite brittleness [24].

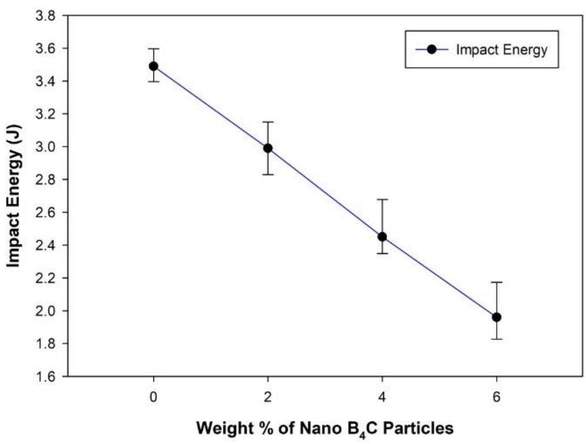

Fig. 13 Impact strength of Zn-Sn alloy and its nano B_4C composites

Impact cracked surfaces of as-cast Zn alloy, Zn-2 wt. per cent, and Zn-6 wt. percent, SEM micrographs Figure 10 depicts B_4C reinforced composites. The Zn-Sn alloy matrix has larger dimples with voids, as shown in Fig. 14 (a), while the matrix alloy tends to have smaller dimples and voids after introducing B_4C particles, as shown in Fig. 14 (b). The soft matrix was turned into a brittle substance by the inclusion of ceramic particles. The impact strength of the newly developed composites is reduced due to strong interfacial bonding between the Zn matrix and B_4C- particles. The impact strength of the newly generated composites is lowered due to strong interfacial bonding between the Zn matrix and B_4C- particles. Brittle materials absorb fewer loads than soft or ductile materials; however, the impact strength of the newly developed composites is reduced. The fracture surfaces of particles reinforced composites containing 2 and 6 weight per cent particles indicate a sharp brittle fracture mode [25].

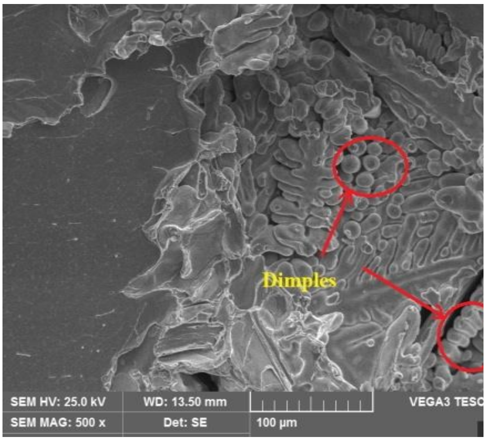

(a)

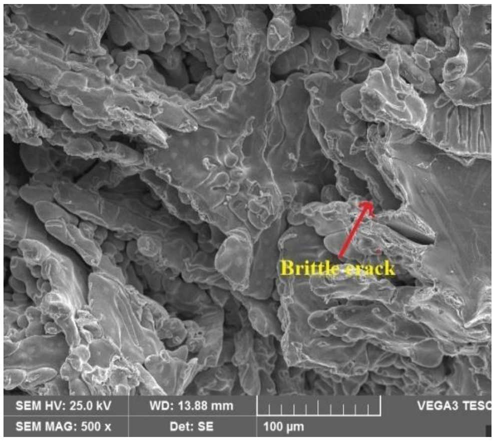

(b)

Fig. 14 Impact fractured surfaces SEM images of (a) as-cast Zn-Sn matrix (b) Zn-Sn alloy matrix with 6 wt. % of B_4C composites

4. Conclusions

A stir casting process was used to make Zn-Sn alloy with 2, 4 and 6 wt. % of B_4C composites. The prepared composites were studied for microstructural characterization by using SEM, EDS and XRD. Scanning electron micrographs were shown the dispersion of boron carbide particles in the Zn-Sn alloy matrix. Further, boron carbide particles in the Zn-Sn alloy matrix were confirmed by the EDS spectrums containing the Boron and Carbon elements, XRD patterns recognized by the Zn, Sn and B_4C phases in the prepared matrix. With the incorporation of nano sized boron carbide particles various mechanical properties like, hardness, ultimate and yield strengths were improved. The percentage improvement in the hardness of Zn-Sn alloy with 6 wt. % of boron carbide particles is 40%. As weight percentage of boron carbide particles were increased to 2 to 6 wt. % in the Zn-Sn alloy, ultimate and yield strengths were improved. Ultimate tensile strength of as-cast Zn-Sn alloy was 315.15 MPa, with 6 wt. % of nano boron carbide particles it was found 394.46 MPa. Addition of hard ceramic particles decreased ductility of Zn-Sn alloy, the lowest ductility was observed in the case of Zn-Sn alloy with 6 wt. % of B_4C particles. Stress-strain patterns of Zn-Sn alloy with boron carbide particles reinforced composites exhibited superior load carrying capacity as compared to the as-cast Zn-Sn alloy. Tensile fractured surfaces of as-cast Zn-Sn alloy indicated the ductile mode of fracture, whereas composites shown brittle fracture. Hard particles addition affected on the impact energy of Zn-Sn alloy, impact strength of Zn-Sn alloy decreased as weight percentage of boron carbide particles increased from 2 to 6 weight percentage in the Zn-Sn alloy. Further, different fracture mechanisms were observed in the case of as-cast Zn-Sn alloy and its boron carbide reinforced composites. Hence, these Zn-Sn alloys with nano born carbide particles composites can be used for future load bearing applications.

References

[1] Nagesh SN, Siddaraju C, Prakash SV, Ramesh MR. Characterization of brake pads by variation in composition of friction materials. Procedia Materials Science, 2014; 5: 295-302. https://doi.org/10.1016/j.mspro.2014.07.270
[2] Manjunatha SS, Manjaiah M, Basavarajappa S. Analysis of factors influencing dry sliding wear behaviour of laser remelted plasma sprayed mo coating using response surface methodology. Achieves of Metallurgy and Materials, 2018; 63 (1): 217-225. https://doi.org/10.1080/17515831.2017.1407473
[3] Dineshkumar S, Sriram S, Surendran R, Dhinakaran V. Experimental investigation of tensile properties of Ti-6Al-4V alloy at elevated temperature. International Journal of Recent Technology and Engineering, 2019; 8(1):103-107.
[4] Prasad GP, Chittappa HC, Nagaral M, Auradi V. Influence of B4C reinforcement particles with varying sizes on the tensile failure and fractography of LM29 alloy composites. Journal of Failure Analysis and Prevention, 2020; 20(6): 2078-2088. https://doi.org/10.1007/s11668-020-01021-6
[5] Ali Z, Muthuraman V, Rathnakumar P, Gurusamy P, Nagaral M. Studies on mechanical properties of 3 wt.% of 40 and 90 μm size B4C particulates reinforced A356 alloy composites. Materials Today: Proceedings, 2022; 52: 494-499. https://doi.org/10.1016/j.matpr.2021.09.260
[6] Anne G, M. Ramesh MR, Shivananda Nayaka, Arya SB, Sahu S. Microstructure evolution and mechanical and corrosion behavior of accumulative roll bonded Mg-2%Zn/Al-7075 multilayered composite. Journal of Materials Engineering and Performance, 2017;26 (4):1726-1734. https://doi.org/10.1007/s11665-017-2576-z
[7] Kumar HSV, Kempaiah UN, Nagaral M. Impact, tensile and fatigue failure analysis of boron carbide particles reinforced Al-Mg-Si (Al6061) alloy composites. Journal of Failure Analysis and Prevention, 2021; 21: 2177-2189. https://doi.org/10.1007/s11668-021-01265-w
[8] Pathalinga PG, Chittappa HC, Nagaral M, Auradi V. Effect of the reinforcement particle size on the compressive strength and impact toughness of LM29 alloy B4C composites. Structural Integrity and Life, 2019;5 (7):231-236.
[9] Nagaral M, Auradi V, Kori SA, Vijaykumar H. Investigations on mechanical and wear behavior of nano Al2O3 particulates reinforced AA7475 alloy composites. Journal of Mechanical Engineering and Sciences, 2019; 13(1):4623-4635. https://doi.org/10.15282/jmes.13.1.2019.19.0389
[10] Harti J, Prasad TB, Nagaral M, Rao KN. Hardness and tensile behavior of Al2219-TiC metal matrix composites. Journal of Mechanical Engineering and Automation, 2016; 6(5A): 8-12.
[11] Ali Z, Muthuraman V, Rathnakumar P, Gurusamy P, Nagaral M. Investigation on the tribological properties of copper alloy reinforced with Gr/ZrO2 particulates by stir casting route. Materials Today: Proceedings, 2020; 33: 3449-3453. https://doi.org/10.1016/j.matpr.2020.05.351
[12] Balaraj V, Nagaraj K, Nagaral M, Auradi V. Microstructural evolution and mechanical characterization of micro Al2O3 particles reinforced Al6061 alloy metal composites. Materials Today: Proceedings, 2021; 47: 5959-5965. https://doi.org/10.1016/j.matpr.2021.04.500
[13] Krishna Prasad S, Samuel Dayanand, Rajesh , Madeva Nagaral, Auradi V, Rabin Selvaraj. Preparation and Mechanical Characterization of TiC Particles Reinforced Al7075 Alloy Composites, Advances in Materials Science and Engineering, 2022,

Article ID 7105189, https://doi.org/10.1155/2022/7105189. https://doi.org/10.1155/2022/7105189

[14] Nagaral M, Auradi V, Kori SA, Reddappa HN, Jayachandran, Shivaprasad V. Studies on 3 and 9 wt. % of B4C particulates reinforced Al7025 alloy composites. In AIP Conference Proceedings, 2017; 1859, 1: 020019. https://doi.org/10.1063/1.4990172

[15] Nagaral M, Deshapande RG, Auradi V, Satish BP, Samuel D, Anilkumar MR. Mechanical and wear characterization of ceramic boron carbide-reinforced Al2024 alloy metal composites. Journal of Bio-and Tribo-Corrosion, 2021; 7(1):1-12. https://doi.org/10.1007/s40735-020-00454-8

[16] Nagara M, Auradi V, Bharath V. Mechanical characterization and fractography of 100 micron sized silicon carbide particles reinforced Al6061 alloy composites. Metallurgical and Materials Engineering, 2022; 28 (1): 17-32. https://doi.org/10.30544/639

[17] Fazil N, Venkataramana V, Nagaral M, Auradi V. Synthesis and mechanical characterization of micro B4C particulates reinforced AA2124 alloy composites. International Journal of Engineering and Technology UAE, 2018; 7 (2.23): 225-229. https://doi.org/10.14419/ijet.v7i2.23.11954

[18] Marco Z, Carlos ES, Alicia EA. Investigation on Al2O3 reinforced zinc aluminium matrix composites. Procedia Materials Science, 2015;8:424-433. https://doi.org/10.1016/j.mspro.2015.04.093

[19] Jeng J, Xu J, Hua W, Xia L, Deng X, Wang S, Tao P, Ma X, Yao J, Jiang C, Lin L. Wear Performance of the lead free tin bronze matrix composite reinforced by short carbon fibers. Applied Surface Science, 2009;255:6647-6651. https://doi.org/10.1016/j.apsusc.2009.02.063

[20] Ferguson JB, Schultz BF, Rohatgi PK. Zinc alloy ZA-8 shape memory alloy self healing metal matrix composite. Materials Science and Engineering A, 2015;620(3):85-88. https://doi.org/10.1016/j.msea.2014.10.002

[21] Halil BK, Hasan U, Ahmet CT, Okan D, Ahmet A. Influence of sea water on mechanical properties of SiO2-epoxy polymer nanocomposites. Research on Engineering Structures and Materials, 2019;5(2):147-154.

[22] Ahmet CT, Halil BK, Hasan U, Okan D, Ahmet A. Evaluation of low-velocity impact behavior of epoxy nanocomposite laminates modified with SiO2 nanoparticles at cryogenic temperatures. Research on Engineering Structures and Materials, 2019;5(2):115-125.

[23] Mei Z, Zhu YH, Lee WB, Yue TM, Pang GKH. Microstructure investigation of a SiC whisker reinforced eutectoid zinc alloy matrix composite. Composite Part A: Applied Science and Manufacturing, 2006;37(9):1345-1350. https://doi.org/10.1016/j.compositesa.2005.08.011

[24] Wenlong Z, Xiang M, Dongyan D. Aging behavior and tensile response of a SiCw reinforced eutectoid zinc-aluminium-copper alloy matrix composite. Journal of Alloys and Compounds, 2017;727:375-381. https://doi.org/10.1016/j.jallcom.2017.08.130

[25]Uppada RK, Putti SR, Mallarapu GK. Mechanical behavior of fly ash-SiC particles reinforced Al-Zn alloy based metal matrix composites fabricated by stir casting method. Journal of Materials Research and Technology, 2019;8(1):737-744. https://doi.org/10.1016/j.jmrt.2018.06.003